Uncovering Ion Transport Mechanisms in Ionic Liquids Using Data Science

(Supplemental Information)

By: J. E. Umaña, Ryan K. Cashen, Victor M. Zavala, and Matthew A. Gebbie*

Department of Chemical and Biological Engineering, University of Wisconsin-Madison, Madison, WI 53706, United States of America

* Corresponding author

Nernst-Einstein Model.

The Nernst-Einstein basis in fundamental theory gives a quantitative prediction of how efficient fully dissociated ions should move in an electrolyte given the bulk viscosity and ion sizes. By comparing the Nernst-Einstein molar conductivity prediction to experimental measurements of the molar conductivity, one can develop a quantitative metric for how ion transport in ionic liquids compares to hydrodynamic Nernst-Einstein predictions (1, 2).

Prior studies have used the Nernst-Einstein approach in combination with databases of ionic liquid properties to indicate that ionic liquids can exhibit conductivities that are either lower or higher than hydrodynamic predictions, depending on how ion sizes are defined (2, 3). However, the Nernst-Einstein model is still one of the simplest theoretical model that captures the general behavior of ionic liquid conductivity, and it remains largely unclear what specific molecular properties control the differences in transport mechanisms that are thought to drive deviation from hydrodynamic predictions of ion mobility.

Ionic Liquid Properties and Molecular Descriptors Descriptions.

2D and 3D RDKit and PubChem descriptors were chosen for our database analyses. We note that RDKit and PubChem do not simulate intermolecular interactions, so all computed descriptors are derived from non-interacting ion conformers. These simulations sample ion conformations for individual ions in vacuum to calculate molecular descriptors for each ion investigated from the ILThermo database. In addition, RDKit and PubChem do not simulate formal charge distributions for electrostatic interaction calculations. Therefore, 3D molecular shape and energetic descriptors contain inaccuracies from the variations in accessible molecular conformers for ions simulated without stabilizing intermolecular forces. Computed 2D molecular descriptors do not depend on simulated intermolecular interactions or formal charges distributions and remain accurate for ionic liquids.

Table S1. Experimental System Descriptors Descriptions

Descriptor Name	Description
Molar Conductivity (4, 5)	Experimentally measured specific conductivity by measured molar concentration.
Temperature (4, 5)	Experimental measurement conditions.
Viscosity (4, 5)	Experimentally measured IL fluid bulk resistance to flow.
Density (4, 5)	Experimentally measured mass per volume.
Heat Capacity (4, 5)	Experimentally measured energy change per temperature change at constant atmospheric pressure.
Melting Point (4, 5)	Experimentally measured temperature of liquid-solid phase equilibrium at atmospheric pressure.

Table S2. Molecular Structure Descriptors Descriptions

Descriptor Name	Description
Atom Count (6)	Number of atoms in each ion.
Bond Count (6)	Number of bonds in each ion.
Rotatable Bond Count (6)	Number of single bonds, not in a ring, bound to a nonterminal heavy atom, excluding amide C-N bonds.
Rotatable Bond Fraction (6)	Rotatable bond counts divided by bond count.
Hydrogen Bond Acceptors (6)	Number of highly electronegative atoms with lone pairs, primarily N, O, and F.
Hydrogen Bond Donor (6)	Number of hydrogens bonded to N, O, or F.
Molecular Weight (6)	Sum of the atomic masses of atoms in an ion.
Valence Electrons (7)	Sum of electrons in the outermost shells of atoms in an ion.

Table S3. Molecular Shape Descriptors Description

Descriptor Name	Description
Volume (8)	Amount of space taken up by an ion. Calculated using PubChem 3D.
Ionic Radius (8)	Radius calculated from volume using the equation for a sphere.
Cation/Anion Volume Ratio (8)	Ratio of cation to anion volume.
Avg. Sphericity (7)	A score of how spherical a molecule is using simulated principal moments of inertia averaged over 50 simulations. $Sphericity = \frac{(PM3 - PM2)^2 + (PM3 - PM1)^2 + (PM2 - PM1)^2}{PM3^2 + PM2^2 + PM1^2}$
Avg. Asphericity (7)	A score of how aspherical a molecule is along its shortest principal moments of inertia using simulated principal moments of inertia averaged over 50 simulations. $Asphericity = \frac{3 * PM1}{PM3 + PM2 + PM1}$
Rel. Std. Dev. Sphericity (7)	Standard deviation of sphericity divided by the mean of sphericity over 50 simulations.
Rel. Std. Dev. Asphericity (7)	Standard deviation of asphericity divided by the mean of asphericity over 50 simulations.

Table S4. Molecular Energetics Descriptors Description

Descriptor Name	Description
Polar Area (6)	Polar surface area of an ion calculated using Cactvs 3.4.8.18.
Hydrogen Bond Donor Interactions (6)	Number of hydrogen bond donors on an ion multiplied by the number of hydrogen bond acceptors on the counter-ion.
LogP (6)	Log_{10} of the octanal-water partition coefficient calculated by XLogP3.(9)
Max. Partial Charge (7)	Highest partial charge on an ion averaged over 50 simulations.
Min. Partial Charge (7)	Lowest partial charge on an ion averaged over 50 simulations.

Dissociation Energies.

Effective ionic liquid pair dissociation energies, E_d [kJ/mol], are calculated using Eqn S1 where E_{DFT} [kJ/mol] is the reported calculated vacuum interaction energy of ionic liquid counter-ions and ε is the low frequency dielectric relative permittivity of the ionic liquid (10).

$$E_d = \frac{E_{DFT}}{\varepsilon} \quad \text{(S1)}$$

t-SNE Maps for Other Properties.

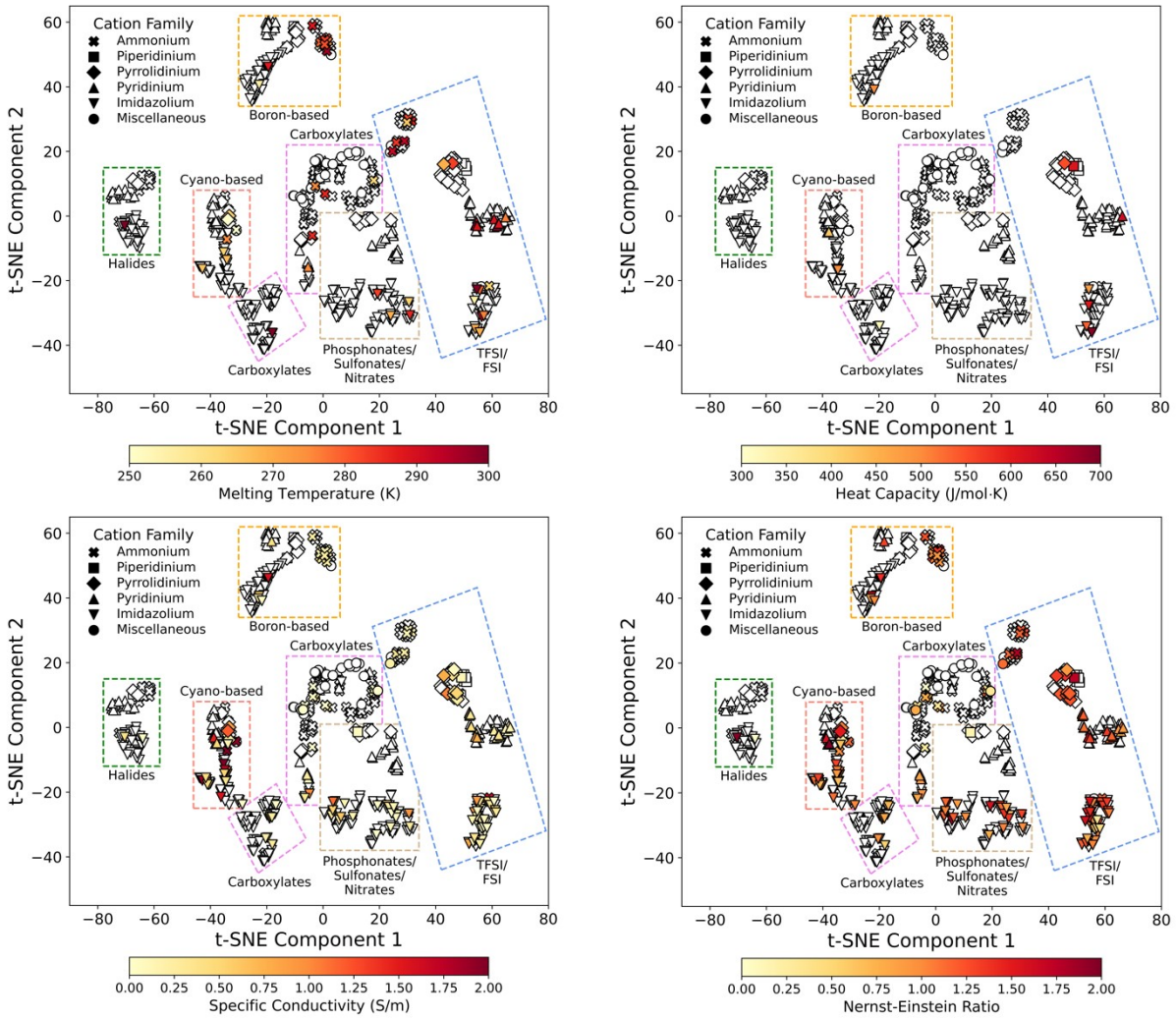

Figure S1. t-SNE projections of molecular similarity overlayed with melting point (top left) at atmospheric pressure and heat capacity (top right), specific conductivity (bottom left), and Nernst-Einstein ratio (bottom right) at 298 K. We observe a sparse correlation between heat capacity and structure and no correlation for other overlayed properties.

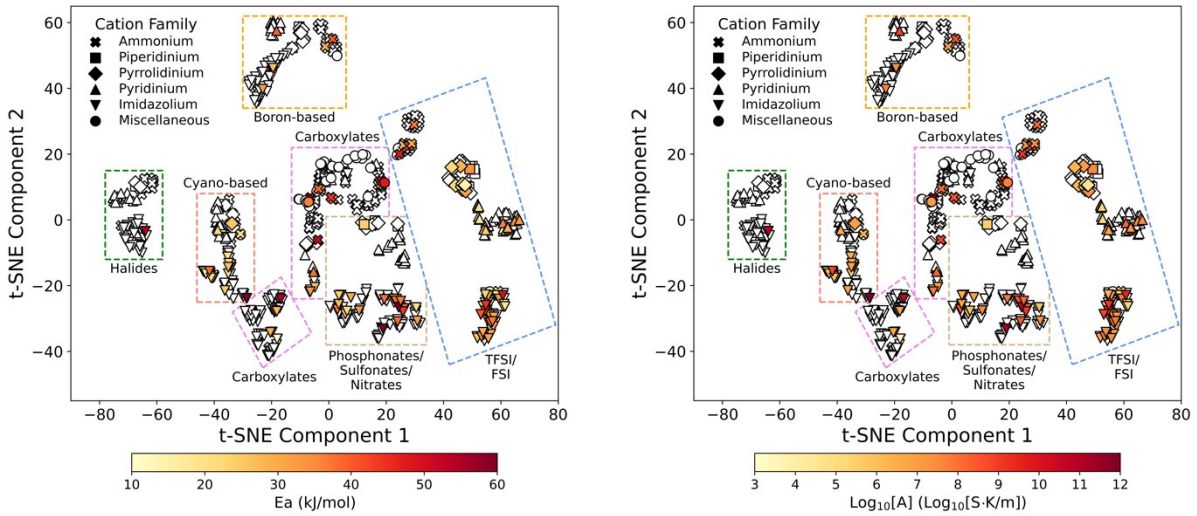

Figure S2. t-SNE projections of molecular similarity overlayed with fit Arrhenius model activation energy (Left) and Log_{10}[frequency factor] (Right).

Hybrid Model Parity Plots.

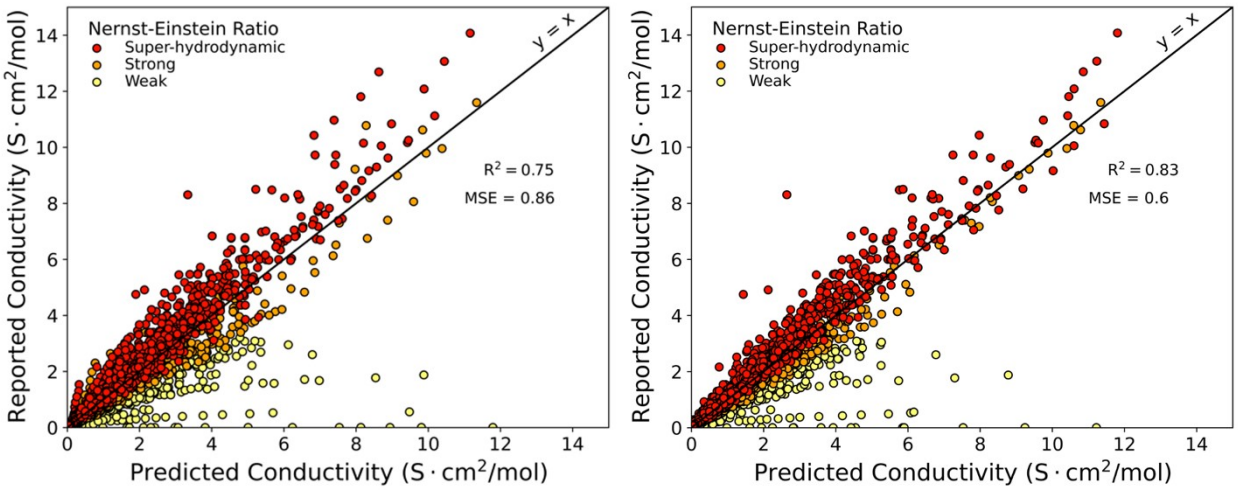

Figure S3. Hybrid model parity plot using only Nernst-Einstein inputs of viscosity, cation radius, and anion radius (left) and hybrid model parity plot using Nernst-Einstein variables, cation polar area, anion hydrogen bond donor count, anion valence electrons, and anion hydrogen bond acceptor count (right). The addition of these RDKit descriptors significantly improves prediction accuracy for high-conductivity ionic liquids but retains the same inaccuracies for "Weak"-labeled ionic liquids. The retention of these outliers indicates that

Ionic Liquid Machine Learning Training Performance.

Table S5. Training set prediction R^2, MSE, and RMSE.

Property	Connectivity Graph	RDKit Descriptors	Bulk Properties	RDKit Descriptors & Bulk Properties
Conductivity (S cm^2/mol)	R^2 = 0.83 MSE = 0.601 RMSE = 0.78	R^2 = 0.97 MSE = 0.109 RMSE = 0.33	R^2 = 0.74 MSE = 0.899 RMSE = 0.95	R^2 = 0.98 MSE = 0.081 RMSE = 0.284
Density (kg/m^3)	R^2 = 0.95 MSE = 1369 RMSE = 37	R^2 = 0.99 MSE = 169 RMSE = 13.0	R^2 = 0.08 MSE = 25047 RMSE = 158	R^2 = 1.0 MSE = 99.2 RMSE = 10.0
Viscosity (Pa s)	R^2 = 0.27 MSE = 0.095 RMSE = 0.31	R^2 = 0.30 MSE = 0.091 RMSE = 0.30	R^2 = 0.27 MSE = 0.095 RMSE = 0.308	R^2 = 0.27 MSE = 0.095 RMSE = 0.308
Heat Capacity (J/mol K)	R^2 = 0.93 MSE = 1203 RMSE = 34.7	R^2 = 0.98 MSE = 264 RMSE = 16.3	R^2 = 0.35 MSE = 11321 RMSE = 106.4	R^2 = 0.89 MSE = 338.4 RMSE = 18.4
Melting Point (K)	R^2 = 0.52 MSE = 157 RMSE = 12.5	R^2 = 0.23 MSE = 249 RMSE = 15.8	R^2 = 0.24 MSE = 248 RMSE = 15.7	R^2 = 0.24 MSE = 245.6 RMSE = 15.7
Residual Conductivity (S cm^2/mol)	R^2 = 0.10 MSE = 0.884 RMSE = 0.94	R^2 = 0.96 MSE = 0.035 RMSE = 0.19	R^2 = 0.04 MSE = 0.95 RMSE = 0.97	R^2 = 0.67 MSE = 0.329 RMSE = 0.57

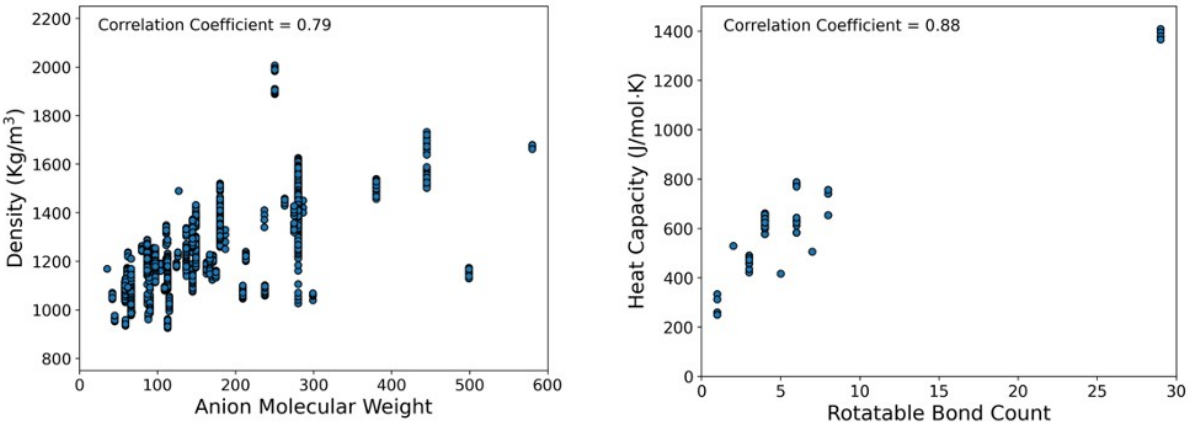

Figure S4. Density vs anion molecular weight (Left) and heat capacity vs rotatable bond count (Right). Each plot depicts strong positive correlations with molecular descriptors and highlights underlying molecular mechanisms. Density in ionic liquids is largely controlled by the anion due to the large atomic mass of inorganic atoms found in ionic liquid anions. Heat capacity is controlled by conformational degrees of freedom and is captured by the number of rotatable molecular bonds.

Ionic Liquid Machine Learning Model Hyperparameters.

Neural network architecture and optimization were identical for all trained neural networks. However, learning rate and epochs were chosen to minimize test set MSE to provide equal comparison across molecular representations. Hyperparameters for each neural network are shown in **Table S6** Training batches were kept constant at 256 for all neural network models.

Table S6. Neural network learning rates (LR) and epochs.

Property	Connectivity Graph	RDKit Descriptors	Bulk Properties	RDKit Descriptors & Bulk Properties
Conductivity (S cm^2/mol)	LR = 2.88e-4 Epochs = 150	LR = 2.88e-4 Epochs = 600	LR = 5.76e-4 Epochs = 1600	LR = 2.88e-4 Epochs = 600
Density (kg/m^3)	LR = 1.44e-4 Epochs = 100	LR = 7.2e-5 Epochs = 1000	LR = 7.2e-4 Epochs = 200	LR = 7.2e-5 Epochs = 1000
Viscosity (Pa s)	LR = 7.2e-5 Epochs = 250	LR = 7.2e-5 Epochs = 130	LR = 1.44e-4 Epochs = 500	LR = 7.2e-5 Epochs = 50
Heat Capacity (J/mol K)	LR = 2.88e-4 Epochs = 200	LR = 7.2e-5 Epochs = 500	LR = 1.44e-4 Epochs = 275	LR = 7.2e-5 Epochs = 300
Melting Point (K)	LR = 1.44e-4 Epochs = 500	LR = 7.2e-5 Epochs = 30	LR = 1.44e-4 Epochs = 200	LR = 3.6e-5 Epochs = 80
Residual Conductivity (S cm^2/mol)	LR = 1.44e-4 Epochs = 300	LR = 7.2e-5 Epochs = 300	LR = 1.44e-4 Epochs = 100	LR = 7.2e-5 Epochs = 300

Arrhenius Parameter Machine Learning Performance.

Since activation energies appear to be a key parameter to collapse viscosity-conductivity scaling relationships in ionic liquids, we test the extent to which our database of ionic liquid descriptors can predict activation energies and pre-exponential factors. Arrhenius parameters were predicted using connectivity graphs, RDKit descriptors, and bulk ionic liquid properties using an artificial neural network. We find that all ionic liquid representations result in poor model accuracies, see model performances in **Table S6.**

Table S6. Test set R^2, MSE, and RMSE values for neural network predictions of modified Arrhenius model parameters E_a and A.

Property	Connectivity GNN	RDKit ANN	Props ANN
E_a (kJ/mol)	R^2 = 0.07 MSE = 89.2 RMSE = 9.4	R^2 = 0.25 MSE = 71.5 RMSE = 8.5	R^2 = 0.35 MSE = 62.1 RMSE = 7.9
Log(A) (Log(S cm^2 K/mol))	R^2 = 0.0 MSE = 1.73 RMSE = 1.3	R^2 = 0.18 MSE = 1.42 RMSE = 1.2	R^2 = 0.25 MSE = 1.31 RMSE = 1.1

Table S7. Training set R^2, MSE, and RMSE values for neural network predictions of modified Arrhenius model parameters E_a and A.

Property	Connectivity GNN	RDKit ANN	Props ANN
Ea	$R^2 = 0.29$	$R^2 = 0.94$	$R^2 = 0.38$
(kJ/mol)	MSE = 68.1	MSE = 5.35	MSE = 58.9
	RMSE = 8.3	RMSE = 2.31	RMSE = 7.7
Log(A)	$R^2 = 0.21$	$R^2 = 0.69$	$R^2 = 0.3$
(Log(S cm^2	MSE = 1.37	MSE = 0.54	MSE = 1.22
K/mol))	RMSE = 1.17	RMSE = 0.73	RMSE = 1.1

We report an inability to predict Arrhenius model parameters using available 2D structure, 3D single-ion descriptors, or bulk ionic liquid properties, due to the inherent dependence of Arrhenius model parameters on molecular interactions for ion transport modeling. We reference the lack of explicit information regarding intermolecular interactions in widely available ionic liquid descriptions as a large source of error in our model. Energetic barriers to ion motion and "hole" formation frequency in ionic liquids cannot be determined by structural or bulk descriptors and instead likely depend on collective ionic interactions.

We suggest that DFT calculations or molecular simulations, in conjunction with the Arrhenius model, may enable a rapid screening of ionic liquid electrolyte candidates. Here, we find that such information is inaccessible using currently available ionic liquid descriptor and bulk property information. However, DFT and molecular simulations could be key in more easily accessing estimated ion Arrhenius parameters via estimated interaction energy and dielectric permittivity.

Activation Energy and Permittivity Data.

Table S8. Ionic Liquid Activation Energies and Available Permittivities

Ionic Liquid	E_a (kJ/mol)	Permittivity (11)
1-ethyl-3-methylimidazolium acetate	37.2	16.3
1-ethyl-3-methylimidazolium Bistriflylimide anion	23.3	13.8
1-ethyl-3-methylimidazolium Cyanoiminomethylideneazanide	20.5	12.5
1-ethyl-3-methylimidazolium trifluoromethanesulfonate	19.9	19.3
1-hexyl-3-methylimidazolium Bistriflylimide anion	31.4	8.5
1-ethyl-3-methylimidazolium thiocyanate	18.1	15.1
1-ethyl-3-methylimidazolium tetrafluoroborate	26.7	12.9
1-butyl-1-methylpyrrolidinium tris(pentafluoroethyl)trifluorophosphate	36.8	5.3
1-butyl-3-methylimidazolium methylsulfate	38.9	11.9
1-butyl-3-methylimidazolium tetrafluoroborate	32.4	9.7
1-butyl-3-methylimidazolium thiocyanate	21.3	9.7
1-butyl-3-methylimidazolium Bistriflylimide anion	28.9	9.2
1-butyl-3-methylimidazolium Cyanoiminomethylideneazanide	23.7	10.3
1-methyl-3-octylimidazolium Bistriflylimide anion	35.3	6.9
1-propyl-3-methylimidazolium Bistriflylimide anion	29.4	9.4
1-propyl-3-methylimidazolium iodide	34.8	5.5
1-hexyl-3-methylimidazolium hexafluorophosphate	43.5	7.1
1-Ethyl-3-methylimidazolium L-lactate	28.2	12.1
1-hexylpyridinium Bistriflylimide anion	33.3	6
1-butyl-1-methylpyrrolidinium Cyanoiminomethylideneazanide	25.3	8.1

Bibliography.

1. O. Nordness, J. F. Brennecke, Ion Dissociation in Ionic Liquids and Ionic Liquid Solutions. *Chem Rev* **120**, 12873-12902 (2020).
2. P. Nurnberg *et al.*, Superionicity in Ionic-Liquid-Based Electrolytes Induced by Positive Ion-Ion Correlations. *J Am Chem Soc* **144**, 4657-4666 (2022).
3. R. K. Cashen, M. M. Donoghue, A. J. Schmeiser, M. A. Gebbie, Bridging Database and Experimental Analysis to Reveal Super-hydrodynamic Conductivity Scaling Regimes in Ionic Liquids. *J Phys Chem B* **126**, 6039-6051 (2022).
4. D. Qian *et al.*, ILThermo: A Free-Access Web Database for Thermodynamic Properties of Ionic Liquids. (2007).
5. A. F. Kazakov, Magee, Joe W., Chirico, Robert D., Diky, Vladimir, Kroenlein, Kenneth G., Muzny, Chris D., Frenkel, Michael D. , Ionic Liquids Database - ILThermo (v2.0). *Ionic Liquids Database - ILThermo (v2.0)* (2013).
6. S. Kim *et al.*, PubChem in 2021: new data content and improved web interfaces. *Nucleic Acids Res* **49**, D1388-d1395 (2021).
7. Anonymous (RDKit: Open-Source Cheminformatics Software.
8. E. E. Bolton *et al.*, PubChem3D: a new resource for scientists. *J Cheminform* **3**, 32 (2011).
9. T. Cheng *et al.*, Computation of Octanol−Water Partition Coefficients by Guiding an Additive Model with Knowledge. *Journal of Chemical Information and Modeling* **47**, 2140-2148 (2007).
10. M. A. Gebbie, H. A. Dobbs, M. Valtiner, J. N. Israelachvili, Long-range electrostatic screening in ionic liquids. *Proc Natl Acad Sci U S A* **112**, 7432-7437 (2015).
11. E. L. Bennett, C. Song, Y. Huang, J. Xiao, Measured relative complex permittivities for multiple series of ionic liquids. *J Mol Liq* **294**, 111571 (2019).